Available online at www.sciencedirect.com
ScienceDirect
Pattern Recognition 41 (2008) 1254–1267
PATTERN RECOGNITION
THE JOURNAL OF THE PATTERN RECOGNITION SOCIETY
www.elsevier.com/locate/pr

A double-threshold image binarization method based on edge detector

Qiang Chen[a,*], Quan-sen Sun[a], Pheng Ann Heng[b,c], De-shen Xia[a]

[a]*The School of Computer Science and Technology, Nanjing University of Science and Technology, Nanjing 210094, China*
[b]*Department of Computer Science and Engineering, The Chinese University of Hong Kong, Shatin, N.T., Hong Kong*
[c]*Shenzhen Institute of Advanced Integration Technology, Chinese Academy of Sciences/The Chinese University of Hong Kong*

Received 22 September 2006; received in revised form 11 May 2007; accepted 10 September 2007

Abstract

This paper presents a new double-threshold image binarization method based on the edge and intensity information. We first find seeds near the image edges and present an edge connection method to close the image edges. Then, we use closed image edges to partition the binarized image that is generated using a high threshold, and obtain a primary binarization result by filling the partitioned high-threshold binary image with the seeds. Finally, the final binarization result is obtained by remedying the primary binarization result with the low-threshold binary image. Compared with the classical binarization methods and the similar binarization methods, our method is effective on the binarization of images with low contrast, noise and non-uniform illumination.

Keywords: Binarization; Double-threshold; Edge connection; Edge detector; Seed filling

1. Introduction

Image binarization is an important preprocessing technology for the recognition of handwritten literal amounts of checks [1,2], document image processing [3–7], recognition of fingerprint images [8], etc. Currently, many binarization methods have been presented, which can be categorized mainly into two classes: global thresholding methods [9–12] and adaptive thresholding methods [13–16]. The global thresholding methods are effective for images with an obviously bimodal histogram. Due to its poor robustness, however, global thresholding methods are not suitable for images with low contrast or non-uniform illumination. Otsu's algorithm [9], a classical global thresholding method, reflects the intensity distribution of an image, but its property of a single threshold results in poor robustness. Although adaptive thresholding methods can deal with some complex images, they often ignore the edge property and lead to a fake shadow. Bernsen's algorithm [13], a classical adaptive thresholding algorithm, computes a separate threshold for each pixel based on the neighborhood of the pixel; so it shows a better adaptation than the global thresholding methods. But it has the limitation of adaptive thresholding methods that when the neighborhood is small, there will be fake shadows and the loss of objects; when the neighborhood is large, the algorithm speed will be greatly decreased. In order to evaluate the performance of binarization methods, Trier and Jain [17] presented a goal-directed evaluation methodology for 19 methods. Eleven different locally adaptive binarization methods were evaluated, and Niblack's method [14] gave the best performance. Sezgin and Sankur [18] evaluated 40 binarization methods based on a combined performance measures, and Kittler's method [11] is the best performing thresholding method in cases of non-destructive testing (NDT) images and document images. Ref. [18] showed that all methods invariably performed poorly for at least one or two images. Thus the combination of thresholding methods can be done at the feature level or at the decision level.

Edge information is useful and has been utilized by several image binarization methods. An image segmentation method that incorporates the global thresholding methods and the edge detecting method was presented in Ref. [19], which made up for the deficiencies of global thresholding methods to some

* Corresponding author. Tel.: +86 25 84315142.
E-mail address: chen2qiang@163.com (Q. Chen).

0031-3203/$30.00
doi:10.1016/j.patcog.2007.09.007

extent. However, it only incorporated the edge information into global thresholding methods, and did not pay enough attention to the intensity of inhomogenous objects. Furthermore, the binarized object boundaries are not smooth enough. Cao et al. [20] proposed a segmentation method of double-sided handwritten archival documents, which obtained the front object region using an improved Canny edge detector, and binarized the object region with Otsu's algorithm. In this method, the edge information was only used to localize the object region, but not to binarize the image. Yanowitz and Bruckstein [15] presented an image segmentation method based on the threshold surface, which is determined by interpolating the image gray levels at points where the gradient is high, indicating probable object edges. Because this method depends completely on the image edge, there exist fake objects when the noise is large or objects loss when the object edges are too weak. Inspired by multiresolution approximation, Blayvas et al. [21] proposed a new way to construct a threshold surface in order to improve the Yanowitz–Bruckstein (YB) method. Compared with the YB method, the binarization with the new threshold surface is comparable.

In this paper, we present a new double-threshold image binarization method, which incorporates the edge image generated by the Canny edge detector. The basic idea is: Firstly, we use the Canny edge detector to generate the edge image, and adaptively obtain a high threshold and a low threshold according to the edge image. Secondly, we set the low intensity pixels, which are close to boundaries and not isolated, as seeds, and then we use the seeds to fill the binarized image generated with the high threshold. The closed edges are regarded as the barrier to seed filling. In addition, we judge whether the current filled region is an object region according to the proportion of the seeds to the boundary pixels in this region. Finally, we remove small regions as noise and obtain the final binarized image.

The rest of the paper is organized as follows. Section 2 presents the theory and implementation of our method. Section 3 describes some important remarks on the implementation of our method in detail. Section 4 compares the performance of our binarization method with those of some binarization methods. Conclusions are drawn in Section 5.

2. Theory and implementation

2.1. Theory

Fig. 1 is a real note image, and Fig. 2 shows the corresponding edge image generated with the Canny edge detector [22]. From Fig. 2, we can see that there are few spurious responses, little loss of important edges, and moreover, edges are considerably complete and smooth. Assuming that the boundaries of actual objects in the edge image are complete and closed, the considerably ideal binarized image (Fig. 3) could be obtained with the seed filling inside the boundaries of the objects. To obtain the binarized result like Fig. 3, we must deal with Fig. 2 as follows: (1) remove spurious edges; (2) close actual edges; (3) fill the object regions. This paper presents a new double-threshold image binarization algorithm according to the consideration above, which considers the favorable properties of the Canny edge detector. The optimality of the detector is related to the following three criteria [23]:

Fig. 1. A note image.

Fig. 2. Edge image.

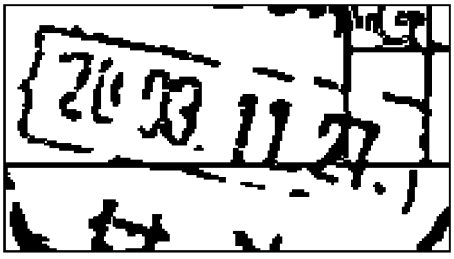

Fig. 3. Manually binarized result.

(1) The detection criterion expresses the fact that important edges should not be missed and there should be no spurious responses.
(2) The localization criterion says that the distance between the actual and located position of the edge should be minimal.
(3) The one response criterion minimizes multiple responses to a single edge.

Some valuable information can be extracted from the edge image, such as the object intensity and the background intensity that are used to determine the high and low thresholds of the image. The extracted seeds should be inside the objects as far as possible, and then we use the seeds to fill the binarized image generated with the high threshold. At the same time, we close the image edges and set the closed image edges as the barrier to the seed filling. In addition, there exists a possibility that seeds grow in background regions, so it is necessary to judge whether the filled region is an object region.

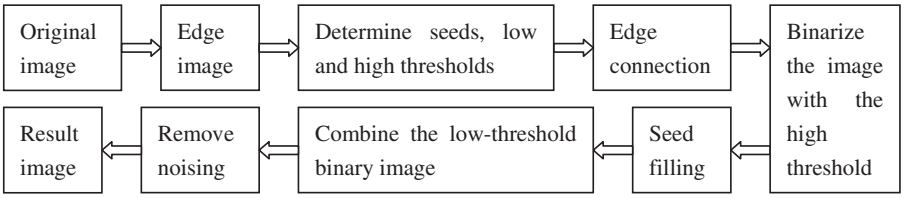

Fig. 4. Block diagram of the proposed algorithm.

2.2. Implementation

According to the theoretical analysis, we obtain the following algorithm in detail:

Step 1: Generate the edge image by using the Canny edge detector.

Step 2: Remove the noise of the original image using the Gaussian filter, and for each edge point of the edge image, take the lowest intensity point within its 8-neighborhood as a seed.

Step 3: Determine the low and high intensity points within the 8-neighborhood of the image edge points, whose gradient magnitudes are larger than the high threshold of the Canny edge detector. Namely, for each edge point with large gradient magnitude, we choose the lowest and the highest intensity points within its 8-neighborhood as the low and the high intensity points, respectively. Take the mean of the high intensity points as the high threshold, and take the mean of the low intensity points as the low threshold. If there is obviously non-uniform illumination in the original image, the high threshold is divided by a weight $l_m \in (0, 1]$ and the low threshold is multiplied by l_m. Otherwise, the high and low thresholds will not be adjusted, or $l_m = 1$.

Step 4: Close the edge image generated in Step 1 by using the edge connection algorithm that will be described in the next section.

Step 5: Binarize the original image with the high threshold, and partition the binarized image with the closed edge image, namely, in the high-threshold binary image generated with the high threshold, we set the pixels that belong to the edge pixels in the closed edge image as background pixels (or white pixels).

Step 6: Use the seeds to fill the partitioned high-threshold binary image generated in Step 5 with the seed-growth algorithm, and for each region generated with the seed-growth algorithm, judge the proportion between the number of the seeds and that of the boundary pixels in the region. If the proportion is larger than a given threshold (in this paper 0.2 is set from experience), the region will be set as an object region. After the seed filling, we obtain a primary binarized result.

Step 7: Combine the primary binarized result with the low-threshold binary image that is generated with the low threshold, namely, in the primary binarized image, we set the pixels that belong to the object regions in the low-threshold binary image as object pixels (or black pixels).

Step 8: Remove the small object region as noise where the number of pixels is less than a given threshold, such as 8, and obtain the final binarized image.

Fig. 4 shows the diagram of the proposed algorithm. Fig. 5 shows the binarization process of Fig. 1 with our binarization algorithm. Fig. 5b shows the edge connection result of Fig. 2. Fig. 5c is the high-threshold binary result, where the high threshold is 144. From Fig. 5c, it can be observed that because the high threshold is large, weak objects with high gray values are detected, but noise and fake shadows are also detected. Fig. 5d shows the result after combining Figs. 5b and c, where actual objects and fake objects are separated by the closed edges. Fig. 5e shows the seeds, where the gray lines are the edges in Fig. 5b, and the white points are the seeds. Fig. 5e demonstrates that seeds are almost within object regions. Fig. 5f shows the result after filling Fig. 5d with the seeds. Fig. 5g shows the binarized result after combining Fig. 5f with the binarized image that is generated with the low threshold 90. Fig. 5h shows the final binarized result. In comparison between Figs. 5h and 3, it is shown that the objects are all detected, but the precision of some details in Fig. 5h is not higher than that in Fig. 3.

3. Remarks

In the following, we present some remarks to explain important steps of our algorithm in detail.

3.1. Establishment of seeds

It is ideal that there are seeds in each object region and there are no seeds in each background region. In order to make each object region have seeds, the lowest intensity point within the 8-neighborhood of each edge point is taken as a seed, which will probably introduce some wrong seeds that are located in background regions. An algorithm for judging the object region will be proposed in order to reduce the influence of wrong seeds in the following subsections. If the edges of an object are too weak to be detected, there will be no seeds in the object region. This influence will be reduced by the low-threshold binary image.

3.2. Generation of the edge image

The edge image is basic to our algorithm, which is used for the separation of objects and backgrounds, selection of seeds and calculation of the high and low thresholds. It is the ideal edge image that separates objects from backgrounds, while there are no spurious edge responses. Spurious responses can result in wrong seeds and inaccurate high and low thresholds. If

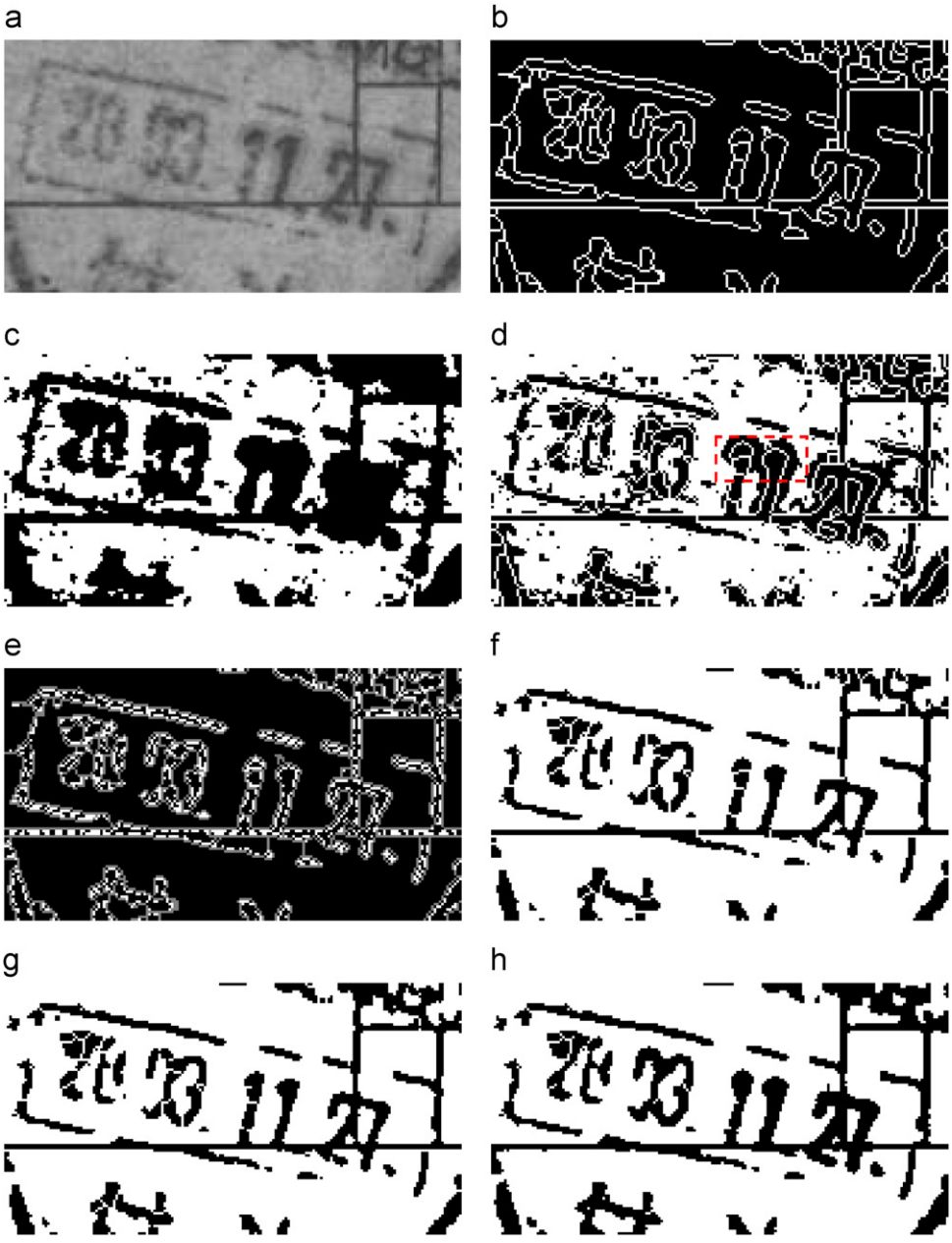

Fig. 5. Implement process of our algorithm: (a) original image; (b) edge connection result; (c) high-threshold binary result; (d) result after combining (b) and (c); (e) seeds; (f) result after filling (d) with the seeds; (g) result after combining (f) with the low-threshold binary image; (h) final binarized result.

we wish that the edge image could completely separate objects and backgrounds, the edge detector should be able to detect weak edges, but this would result in spurious edge responses. In order to overcome the problem, a closed Canny edge image is used to separate objects from backgrounds, and the edges with large edge magnitudes are used to calculate the high and low thresholds. In order to reduce the effect of spurious edge responses on the high and low thresholds, the edges with small edge magnitudes are not used to calculate the high and low thresholds.

Because the disjointed contours will affect the separateness between objects and backgrounds, we connect the disjointed contours of the edge image generated with Canny edge detector to obtain closed contours. Ref. [20] proposed an edge connection method based on edge orientation constraint, which gives no consideration to the distance between the unconnected end points and other edge points. The edge connection method in Ref. [24] is to find the nearest boundary element which is within a half circle for each unconnected end of an open contour. This method considers the distance between edge points, but considers the edge orientation very roughly. This paper presents a new edge connection method, which considers the distance and the edge orientation properly. We categorize the disjointed edges into two cases: isolated points

5	4	3	4	5
4	2	1	2	4
3	1	P	1	3
4	2	1	2	4
5	4	3	4	5

Fig. 6. Template $T0$.

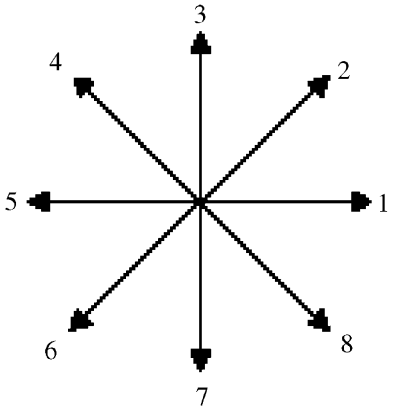

Fig. 7. Eight edge directions.

and non-isolated points, and will discuss them respectively as follows.

3.2.1. Connection of isolated points

Because the isolated point has no edge orientation, we only consider the distance property. Let P be an isolated edge point, a neighborhood is defined as a circle with its center located at P and a search radius r. The nearest edge point which is within the circle, Q, is identified, and then we connect the points P and Q with line generating algorithm. Fig. 6 shows the search template $T0$ with the radius 2. The numbers in the template denote the distance order with P. The smaller the number is, the shorter the distance is.

3.2.2. Connection of non-isolated points

For the connection of non-isolated points, the orientation and the distance properties of edge points are considered, and Fig. 7 shows the 8 edge directions. Let the current non-isolated end point of an edge be P, and P's neighboring and connected edge point be $P1$. We calculate the direction angle θ of the vector $\overrightarrow{P-P1}$, and take one of the 8 directions, which forms the smallest angle with θ as the approximate direction for the point P. For the end point P with some direction, we first search the nearest edge points in the neighborhood with a radius r. Then if there exist several nearest edge points that have the same distance with P, the point that has the smallest angle with P is regarded as the nearest point. Fig. 8 shows the search templates $T1$–$T8$ with a radius 2 which are corresponding to the 8 edge directions, namely, template Ti is corresponding to the i edge direction, where $i = 1, 2, \ldots, 8$. The value in each template represents the order of connection with P. The smaller the value is, the higher the priority of connection with P is. In the following, we will introduce the generation of template with an example of $T1$.

Fig. 9 shows the generation of template $T1$. Let point P be the origin, and point Q be any point in template $T1$. The Euclidean distance between Q and P is $r = \|\overrightarrow{Q-P}\|_2$, where $\|\cdot\|_2$ denotes the 2-norm of a vector. The angle between the vector $\overrightarrow{Q-P}$ and the edge direction 1 is α, where $\alpha \in [0, \pi]$. The order value of connecting Q with P is $d = r^2 + \frac{\alpha}{\pi}$. Similarly, the other order values in template $T1$ can be calculated. Then, the template $T1$ in Fig. 8 is generated by numbering all points in $T1$ according to their order values. The generation of templates Ti, $i = 2, 3, \ldots, 8$, is similar to that of $T1$.

In a summary of the two cases above, we give the following edge connection algorithm for each unconnected edge point P:

(1) Choose one of the 9 templates for the point P according to the two cases above. The criteria of choosing template is that if the point P is an isolated point, template $T0$ is chosen; otherwise, we choose one of the other templates Ti, $i = 1, 2, \ldots, 8$, according to the 8 approximate directions.
(2) According to the template and the edge image, choose the edge point with minimum order value in the template as the nearest point with P. In order to prevent the point P from connecting with the edge points that are close to and connected with P, these $k(k < r)$ edge points in the template are changed to non-edge points before choosing the edge point.
(3) Connect the nearest point with P using line generating algorithm.

In this paper, the template radius is taken to be 10. This process is repeated twice, and all salient open contours will be closed. If there are non-edge points for the unconnected edge point P in the template, we should enlarge the template radius in order to find some edge points in the new template. In this paper, we do not adopt the template with a larger radius to deal with these edge points that are badly unconnected.

3.3. Selection of the high and low thresholds

The high threshold is used to detect all objects, including weak objects with high gray values. The low threshold is used to detect obvious objects with low gray values, without backgrounds. In this paper, the high and low thresholds are calculated according to the edges with large edge magnitudes, and experimental results demonstrate the effectiveness of our method.

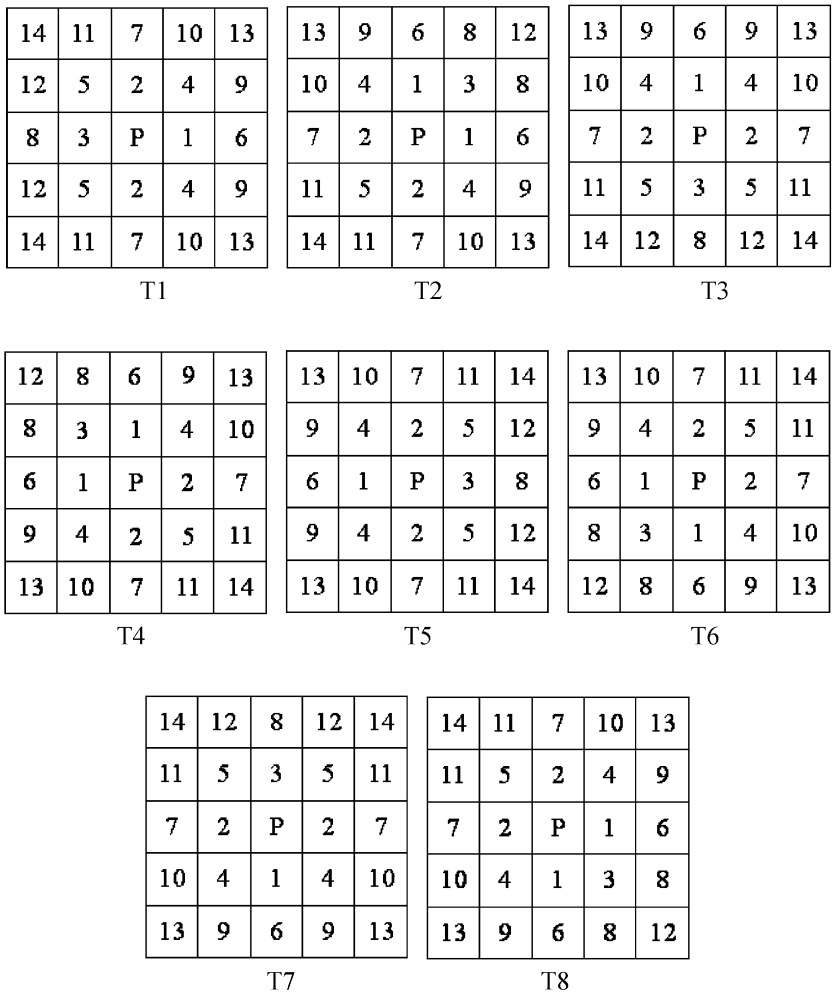

Fig. 8. Eight search templates corresponding to the 8 edge directions.

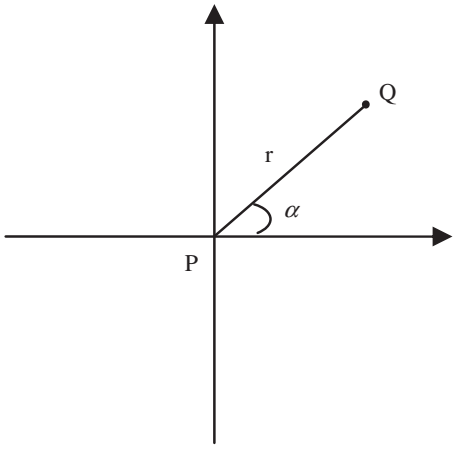

Fig. 9. The generation of template $T1$.

If there is obviously non-uniform illumination in the original image, namely there are object regions with very high intensity or background regions with very low intensity, then we adjust the high and low thresholds with the weight l_m. The purpose of the threshold adjustment is to contain all actual object regions in the high-threshold binary image, but not to contain any background regions in the low-threshold binary image. When l_m is very little (close to 0), the high threshold will be very large (probably be larger than 255, and the high-threshold binary image will be completely black) and the low threshold will be very small (probably be close to 0, and the low-threshold binary image will be completely white). In this case, our algorithm will be similar to the binarized process described in Section 2.1, namely searching object regions in the closed edge image. In the following, we will analyze the selection of the high and low thresholds with an example of a synthetic image.

Fig. 10a shows a synthetic image of 200 × 200 pixels. The gray values in the object and the background both decrease from the left to the right, and the intensity distributions of the object and the background are intersected, which are shown in Fig. 10b. The gray plane in Fig. 10b is the lowest intensity plane of the background, and the intensity distribution of the object above the gray plane lies in the intensity distribution of the background. By using our method, the high and low thresholds are 217 and 156, respectively, where the weight $l_m = 1$. In the following, we will analyze the rationality of the calculated high and low thresholds.

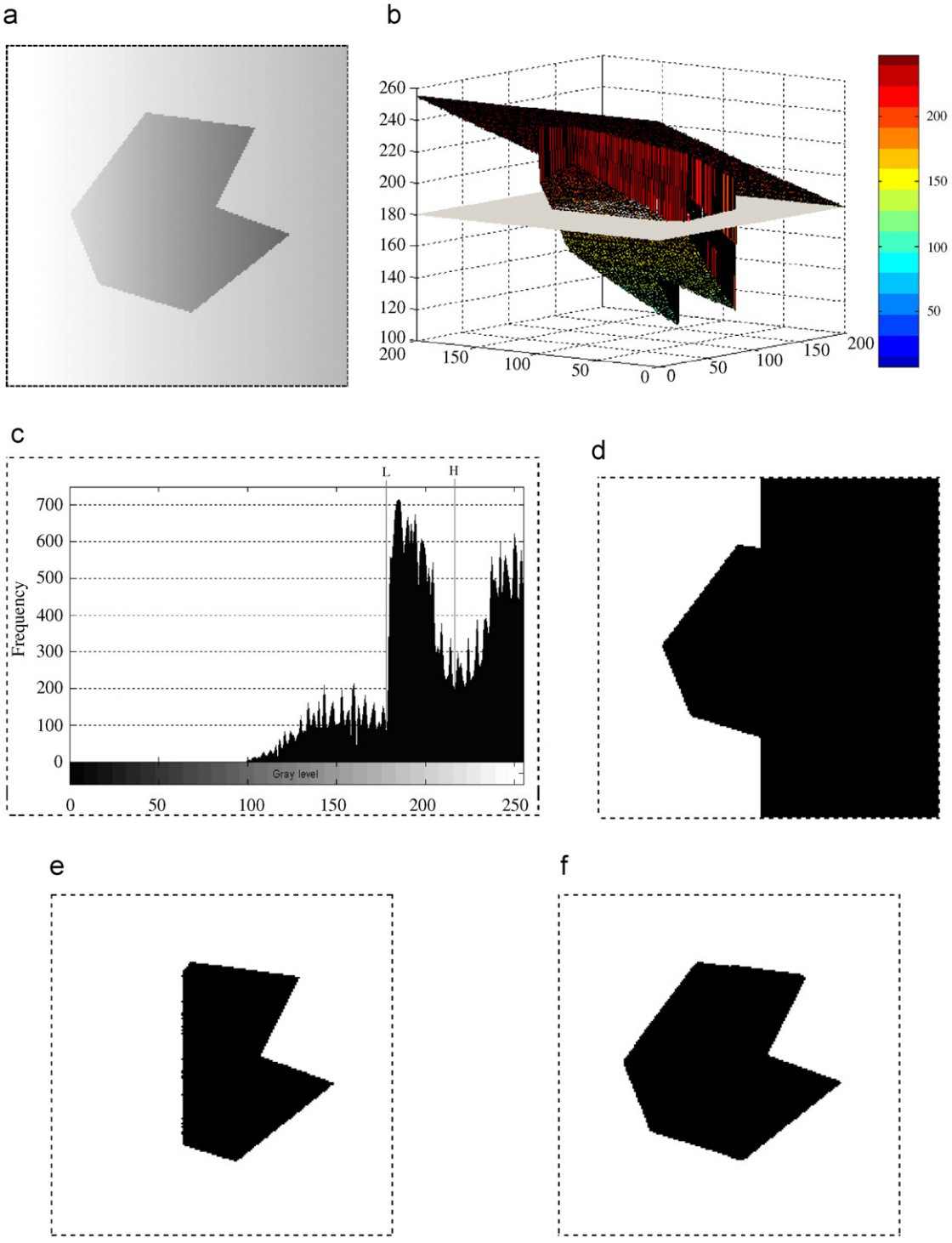

Fig. 10. Selection of the high and low thresholds: (a) a synthetic image; (b) intensity distribution; (c) histogram; (d) binarized result with the high threshold H; (e) binarized result with the low threshold L; (f) binarized result with our method.

Fig. 10c shows the histogram of the image Fig. 10a, in which there exist two valley locations, denoted by $H = 219$ and $L = 179$. Figs. 10d and e show the binarized results with the thresholds, H and L, respectively. After analyzing, it can be known: (1) If the high threshold is smaller than H, there will be object loss in the high-threshold binary image, so that objects will not be completed in the final binarized result. (2) If the high threshold is larger than H, more backgrounds will be detected as objects in the high-threshold binary image, but objects will not be lost. (3) If the low threshold is larger than L, backgrounds will be detected as objects in the low-threshold binary image, so that backgrounds will probably appear in the

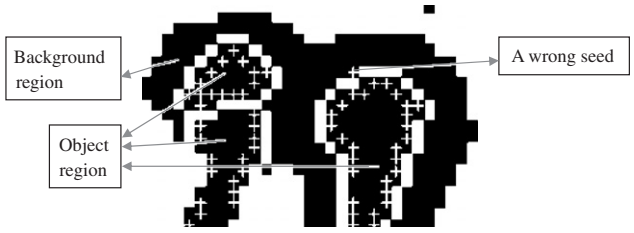

Fig. 11. The distribution of the seeds in the red rectangle region of Fig. 5d.

final binarized result. (4) If the low threshold is smaller than L, fewer objects will be detected in the low-threshold binary image, but backgrounds will not be detected. In the cases of (2) and (4), the final binarized result will not be greatly influenced if the edge image is fine. Therefore, it is ideal for Fig. 10a to set the high and low thresholds as H and L, respectively. The high and low thresholds calculated with our method are close to the ideal values. For our high threshold is set a little bit smaller than H, a part of the object, namely the left corner of the object, is lost in the final binarized result (Fig. 10f).

Therefore, the basic principle of selecting the high and low thresholds is that the high threshold should be set large enough so that all objects would be detected, while the low threshold should be set small enough so that no backgrounds would be detected.

3.4. Judgment of the object region

In Step 6 of our algorithm, the filled region is judged to remove the background region as seeds grow. Because all seeds lie in region boundaries, and mostly lie in object boundaries, the proportion between the number of seeds and that of boundary points is large for a filled object region, but small for a filled background region. Fig. 11 shows the distribution of seeds in the red rectangle region of Fig. 5d, where the seeds are represented by the symbol '+'. From Fig. 11, it can be seen that most of the seeds lie in object regions, and only a small portion of the seeds lie in background regions, so the proportion between the number of seeds and that of boundary points in the object region is larger than that in the background region.

3.5. Measurement of non-uniform illumination

In our algorithm, the judgment of non-uniform illumination depends on the observer. In addition, this paper also presents an approximate measurement of non-uniform illumination, which is based on the analysis of the intensity distribution of edge pixels. The detailed measurement of non-uniform illumination is as follows:

Let I be the original image, and $\{e_i\}, i = 1, \ldots, n$ be the set of the edges with large edge magnitudes in I, where n is the number of edges. Let $\{I_1^i, I_2^i, \ldots, I_{li}^i\}$ be the pixels in the edge e_i that are ascendingly ordered by the intensity, where li is the number of the edge point. The degree of non-uniform illumination d of the image I is

$$d = \frac{1}{m} \cdot \sum_{i=1}^{n} \left((I_{li}^i - I_1^i) - \sum_{j=2}^{li} (I_j^i - I_{j-1}^i)^2 \right),$$

where m is the total number of edge pixels, and I_j^i denotes the intensity of the jth pixel in the edge e_i. The above formula mainly consists of two parts: the intensity range of each edge $(I_{li}^i - I_1^i)$ and the speed of the intensity change $\sum_{j=2}^{li} (I_j^i - I_{j-1}^i)^2$. When there is obvious non-uniform illumination, the intensity range of each edge should be large and the speed of the intensity change should be slow. When there is no obvious non-uniform illumination, generally the intensity range of each edge should be small, or the intensity change of some edges should be abrupt. Therefore, when the value of d is large, there is obvious non-uniform illumination and vice versa.

3.6. Processing of the edge pixels

Seeds grow in the high-threshold binary image that is partitioned by the closed edge image, such as Fig. 5d, so the filled result does not include edge pixels, such as Fig. 5f. In order to make objects more complete, we take the edge pixels, whose gray values are lower than the average of the high and low thresholds, as object pixels.

4. Experimental results and analysis

We make the performance comparison between our method and the classical binarization methods (such as Otsu's method or Bernsen's method) and YB's method which is similar to our method. The experimental images are scanned note images, degraded document images, NDT images and artificial images.

Fig. 12 shows a comparison between some binarization methods with a scanned note image. In the note image, the object intensity is inhomogeneous and there exists fake shadow near the object boundaries. As shown in Fig. 12b, the global thresholding method, Otsu's method, seeks a fine trade-off between the object loss and the noise increase but cannot resolve the conflict between them. The adaptive thresholding methods, Bernsen's method and Niblack's method, are better than Otsu's method. The two adaptive thresholding methods can get more details than Otsu's method, but their robustness is not very good and the object boundaries are coarse, as shown in Figs. 12c and d. For Bernsen's method and Niblack's method, if the width of the window is too small, there will be fake shadow and loss of some object pixels; but if the width of the window is too large, local adaptive threshold will become meaningless and the speed of the algorithm will be decreased greatly. Thus how to select a proper width of the window is a problem to some adaptive thresholding methods. The comparison between Figs. 12e and f shows that our method and YB's method have similar binarization results, and they both overcome the problems that exist in Figs. 12b–d. Therefore, the image binarization methods with the edge information are effective for low contrast note images, which have the properties: less loss of object informa-

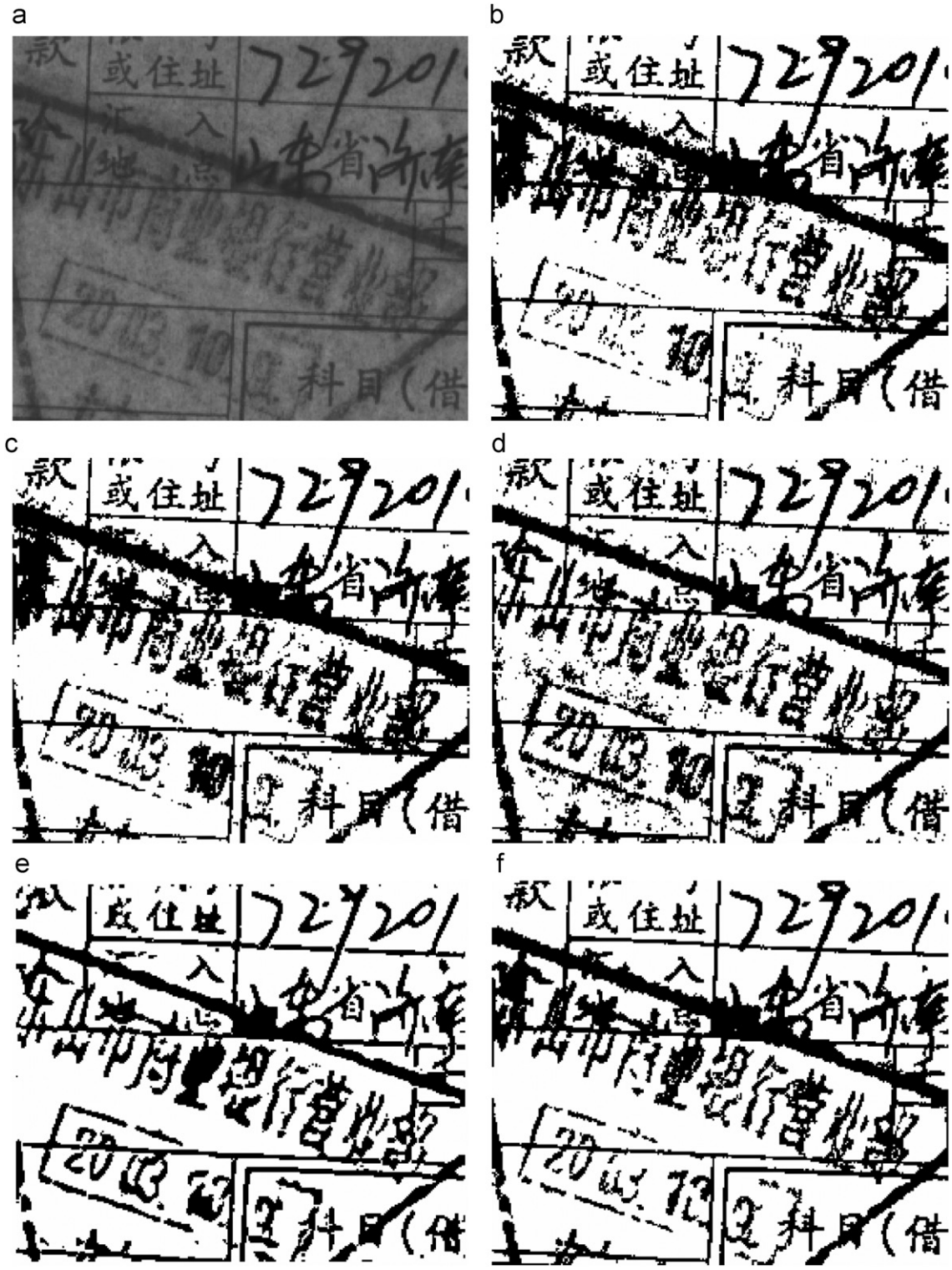

Fig. 12. Comparison between some binarization methods with a scanned note image: (a) original image; (b) Otsu's method; (c) Bernsen's method; (d) Niblack's method; (e) Yanowitz–Bruckstein's method; (f) our method.

tion, good robustness and the smoother object boundary. Most important, they can overcome the influence of fake shadows that often exist in scanned note images.

Fig. 13 shows a comparison between several binarization methods with four degraded document images in which there exist non-uniform illumination, low contrast and smear.

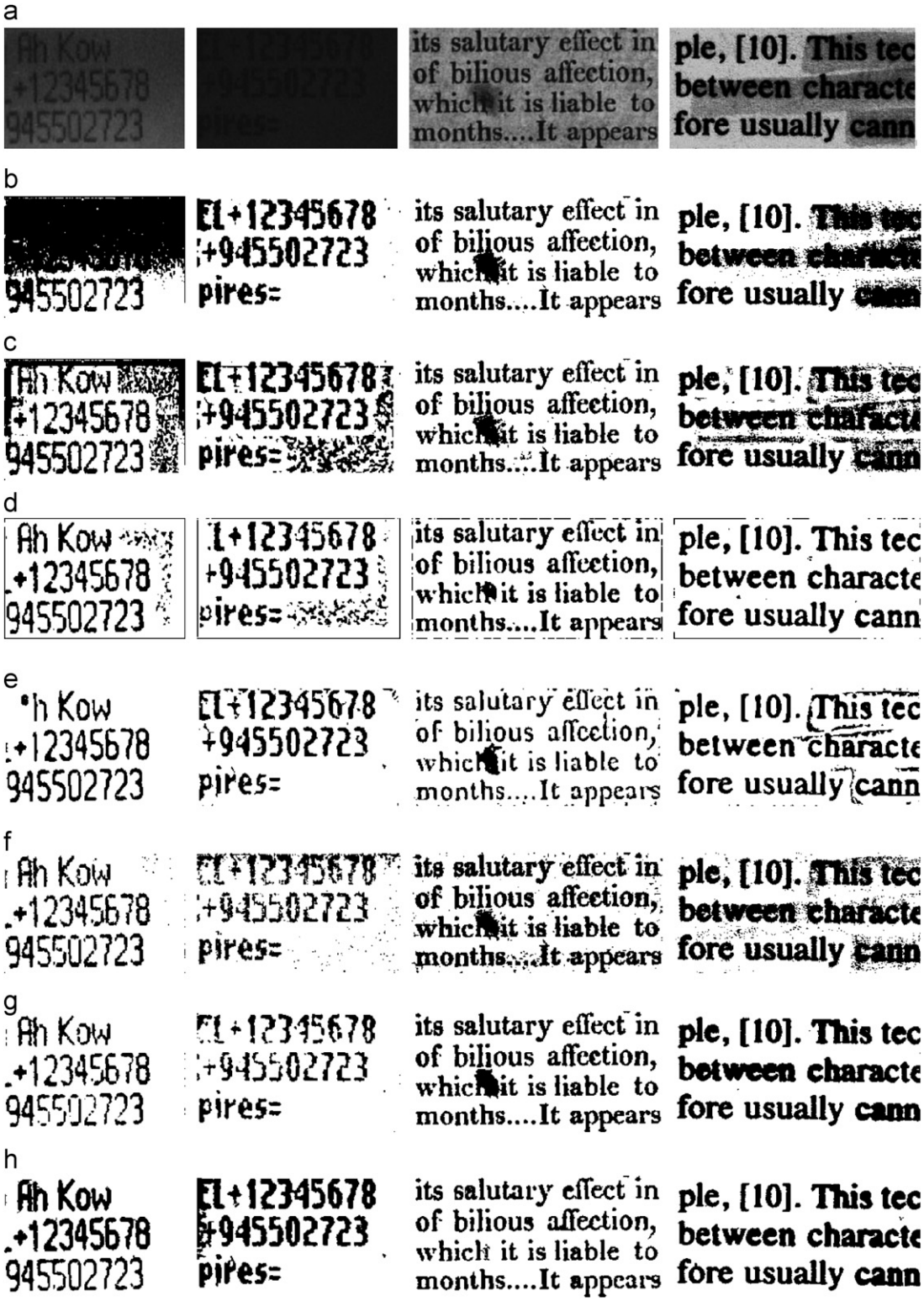

Fig. 13. Comparison between some binarization methods with four degraded document images: (a) four degraded document images; (b) Otsu's method; (c) Bernsen's method; (d) Niblack's method; (e) Yanowitz–Bruckstein's method; (f) Sauvola's method; (g) Gatos's method; (h) our method.

These degraded document images are from other literatures. Figs. 13b–h show the binarized results with Otsu's method, Bernsen's method, Niblack's method, YB's method, Sauvola's method, Gatos's method and our method, respectively. Note that all methods invariably performed poorly for at least one or two images; thus, it can be observed that any single algorithm could not be successful for all image types, even in a single application domain. But for the degraded document images,

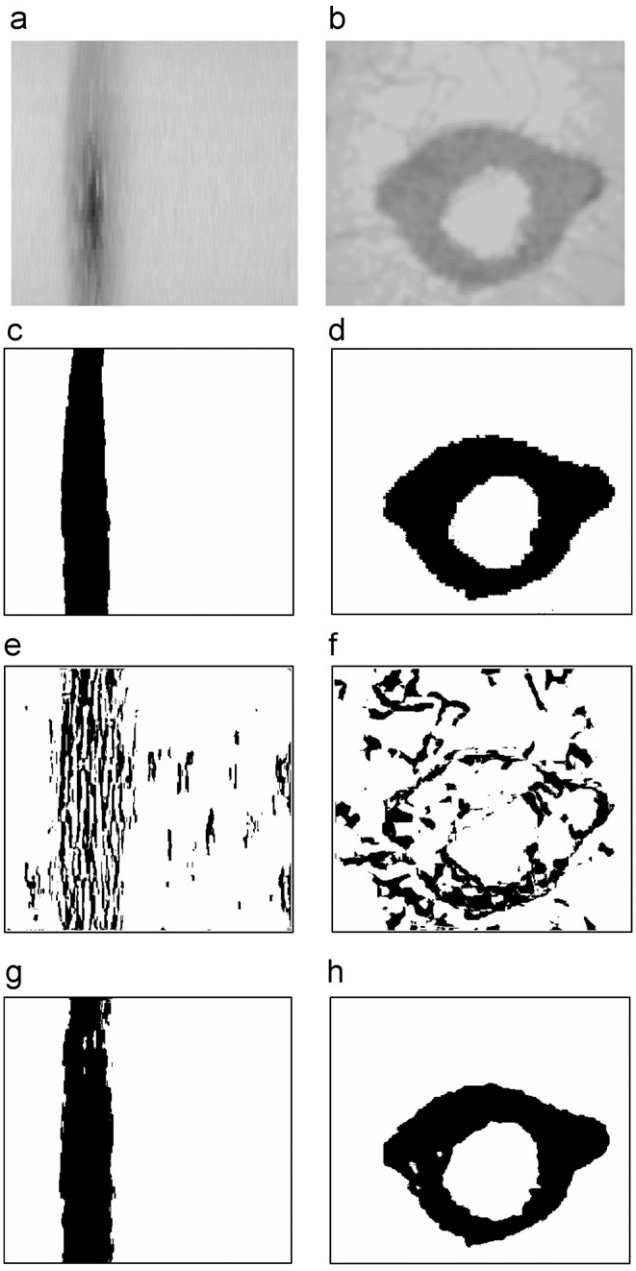

Fig. 14. Comparison between our method and Yanowitz–Bruckstein's method: (a) defective tile image; (b) eddy current image; (c) ground truth result of Fig. 14a; (d) ground truth result of Fig. 14b; (e) binarized result of Fig. 14a with Yanowitz–Bruckstein's method; (f) binarized result of Fig. 14b with Yanowitz–Bruckstein's method; (g) binarized result of Fig. 14a with our method; (h) binarized result of Fig. 14b with our method.

generally, adaptive thresholding methods are better than the global thresholding method, and the average performance of our method is better than those of the others. For the detail of some characters, such as the characters 'a' and 'e', the binarized result with our method is not very good. The binarized results with Gatos's method depend on the binarized results with Sauvola's method to a great extent, because the background surface estimation of Gatos's method is based on the binarized result with Sauvola's method, and the final

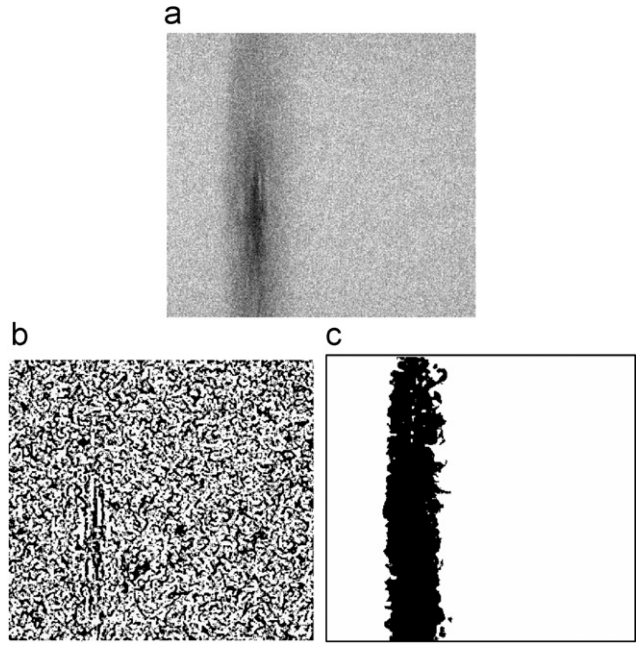

Fig. 15. Robustness comparison between our method and Yanowitz–Bruckstein's method: (a) defective tile image with Gaussian noise; (b) Yanowitz–Bruckstein's method; (c) our method.

binarized result lies on the background surface. Because there are too many parameters in the post-processing process of Gatos's method and the final binarized result is sensitive to these parameters, experimental results show that the binarized results with the post-processing are not better than the results without the post-processing. Thus, for Gatos's method the post-processing is not adopted in this paper.

Fig. 14 shows a comparison between our method and YB's method. In order to generate comparable results, we both adopt the 3×3 mean filter to smooth the original image, and use the same Canny edge detector to determine the image edges. For Fig. 14a, the high and low thresholds are 0.0625 and 0.025, respectively, and for Fig. 14b the high and low thresholds are 0.0781 and 0.0313, respectively. The experimental images are two NDT images used in Ref. [18], a defective tile image (Fig. 14a) and a defective eddy current image including aircraft fuselages (Fig. 14b). Figs.14c and d show the ground truth results. Figs.14e and f show the binarized results with YB's method, where the post-processing step of ghost-elimination was omitted, for the results of the post-processing step are the inverse of Figs.14e and f, respectively. Figs.14g and h show the binarized results with our method. The comparison between Figs.14e–h and the ground truth results (Figs. 14c and d) shows that our method is better than YB's method when the object boundaries are very weak. Because YB's method completely depends on the edge information, objects will lose when the object boundary is too weak to be detected. Even that the object with weak boundaries can be detected by the threshold surface, it would be probably removed by the post-processing step, because there is a small average gradient value at the edge of the object. Though our method may also lose the object during the

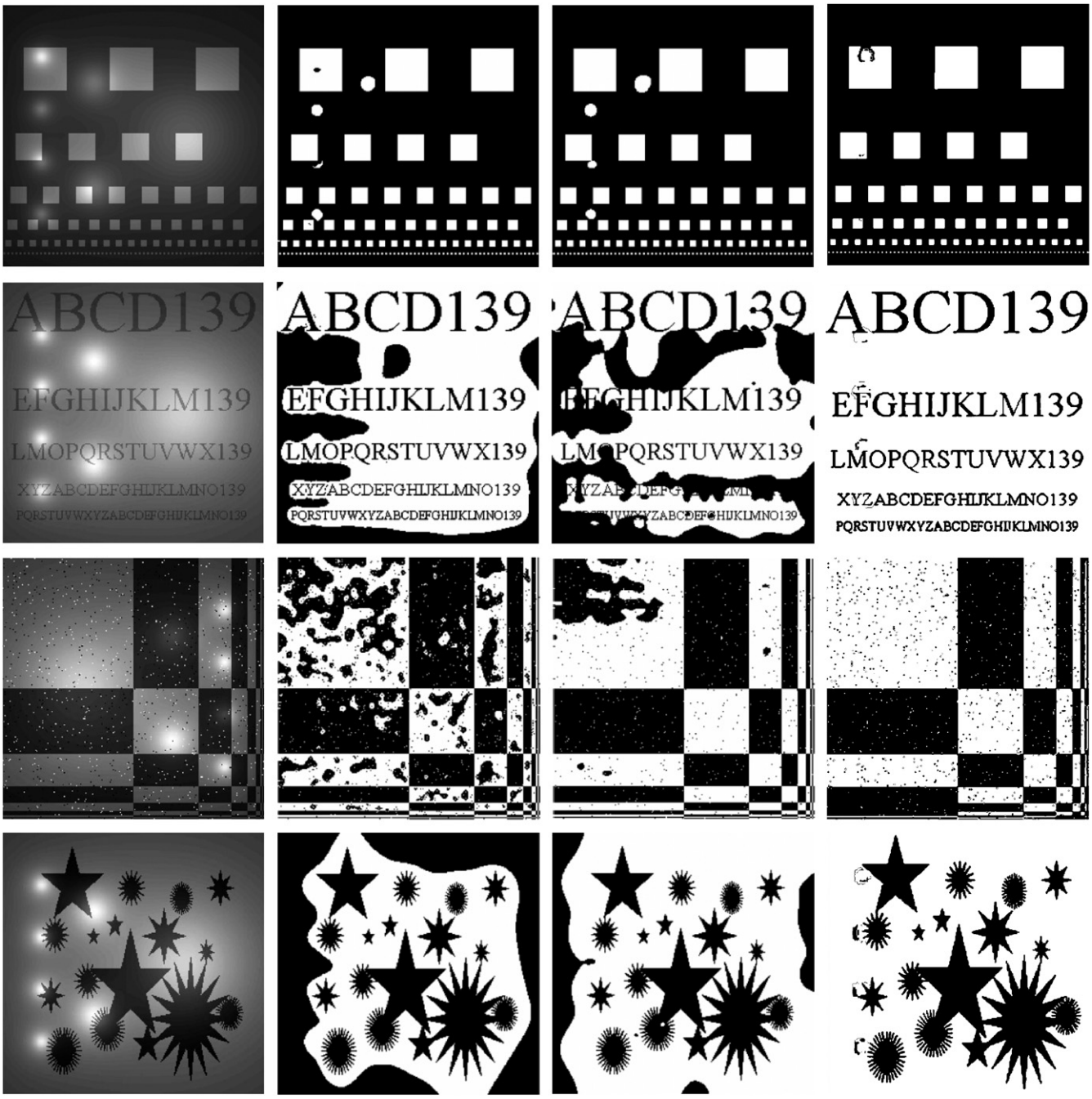

Fig. 16. Binarized results of four artificial images with simulating non-uniform illumination. The first column is the original images; the second column and the third column are the binarized results with YB method and MA method, respectively; the last column is the binarized results with our method.

seed filling due to the loss of object boundaries, obvious object loss can be restored by remedying with the low-threshold binary image.

Fig. 15 shows the robustness comparison between our method and YB's method. Fig. 15a is the defective tile image with Gaussian noise. Figs.15b and c are the results of YB's method and our method, respectively. From Figs. 15b and c, we can observe that the high-threshold binary image can remove most background pixels, so many seeds near spurious edge response will not grow. Therefore, our method has better robustness than YBs' method.

Fig. 16 shows four artificial black–white images generated by simulating non-uniform illumination of the black and white pattern [21]. The binarized results of YB method and multi-resolution approximation (MA) method are from [21]. The misclassification error (ME) [18] is adopted to measure the performance. For the two-class segmentation problem, ME can be expressed as $ME = 1 - \frac{|B_0 \cap B_T| + |F_0 \cap F_T|}{|B_0| + |F_0|}$, where B_0 and F_0 denote the background and foreground of the original (ground-truth) image, respectively, B_T and F_T denote the background and foreground area pixels in the test image, respectively, and $|\cdot|$ is the cardinality of the set. The ME reflects the percentage

Table 1
Comparison of the performance of the YB and MA methods

Method	Test image			
	'Squares'	'Text'	'Rectangles'	'Stars'
YB	0.0063	0.212	0.191	0.312
MA	0.0072	0.312	0.078	0.096
Ours	0.0036	0.0228	0.0639	0.003

of background pixels wrongly assigned to the foreground, and conversely, that of foreground pixels being wrongly assigned to background. The ME varies from 0 for a perfectly classified image to 1 for a totally wrong binarized image.

Due to the obviously non-uniform illumination in Fig. 16, the weight l_m is set to be 0.4. Table 1 presents the binarization errors ME for each method, which demonstrates that the performance of our method is better than those of the YB method and the MA method under different foreground and background conditions.

5. Conclusions

Aiming to overcome the deficiencies of some binarization methods (such as Otsu's method and Yanowitz–Bruckstein's method), including the loss of object information, coarse boundary, poor robustness, etc., this paper presents an automatic double-threshold image binarization method based on the edge detector. The high and low thresholds are based on the edge image. In this paper, we present the basic principle of selecting the high and low thresholds, and analyze the effect of the high and low thresholds. The edge image is mainly used for the separation of objects and backgrounds, selection of seeds and calculation of the high and low thresholds. In order to improve the separation of objects and backgrounds, a new edge connection method, which considers the distance and the edge orientation properly, has been proposed. Based on the analysis of the intensity distribution of edge pixels, an approximate measurement of non-uniform illumination is deployed. In order to remove the background region where wrong seeds grow, the judgment of the object region is proposed based on the proportion between the number of seeds and that of boundary points in the region.

Our method was tested with scanned note images, degraded document images, non-destructive testing images and artificial images. The test results show that our method has several good properties, such as less loss of object information, and high robustness, and has better overall performance than several classic binarization methods.

Acknowledgment

This work was supported by CUHK Direct Grant under Project 2050345. This research was also supported by the National Science Foundation of China under grant no. 60773172.

References

[1] J.C. Simon, O. Baret, N. Gorski, A system for the recognition of handwritten literal amounts of checks. in: Proceedings of the Conference on Document Analysis system, Kaiserslautern, Germany, 1994, pp. 135–155.
[2] H.G. Zhang, G. Chen, G. Liu, J. Guo, Bank check image binarization based on signal matching. in: Fifth International Conference on Information, Communications and Signal Processing, 2005, pp. 1430–1433.
[3] M. Kamel, A. Zhao, Extraction of binary character/graphics images from grayscale document images, Graph. Models Image Process 55 (3) (1993) 203–217.
[4] Ø.D. Trier, T. Taxt, Evaluation of binarization methods for document images, IEEE Trans. Pattern Anal. Mach. Intell. 17 (3) (1995) 312–315.
[5] B. Gatos, I. Pratikakis, S.J. Perantonis, Adaptive degraded document image binarization, Pattern Recognition 39 (3) (2006) 317–327.
[6] Y.B. Yang, H. Yan, An adaptive logical method for binarization of degraded document images, Pattern Recognition 33 (5) (2000) 787–807.
[7] H.H. Oh, K.T. Lim, S.I. Chien, An improved binarization algorithm based on a water flow model for document image with inhomogeneous backgrounds, Pattern Recognition 38 (12) (2005) 2612–2625.
[8] J.H. Li, X.M. Ma, C.A. Guo, Binarization method of fingerprint images based on orientation and dynamic threshold, J. Dalian Univ. Technol. 42 (5) (2002) 626–628.
[9] N. Otsu, A threshold selection method from gray-level histograms, IEEE Trans. Syst. Man Cybernet. 9 (1) (1979) 62–66.
[10] J.N. Kapur, P.K. Sahoo, A.K. Wong, A new method for gray-level picture thresholding using the entropy of the histogram, Comput. Vision Graphics Image Process. 29 (3) (1985) 273–285.
[11] J. Kittler, J. Illingworth, J. Foglein, Minimum error thresholding, Pattern Recognition 19 (1) (1986) 41–47.
[12] M. Cheriet, J.N. Said, C.Y. Suen, A recursive thresholding technique for image segmentation, IEEE Trans. Image Process. 7 (6) (1998) 918–921.
[13] J. Bernsen. Dynamic thresholding of gray-level images, in: Proceedings of the Eighth International Conference on Pattern Recognition, Paris, IEEE Computer Society Press, France, 1986, pp. 1251–1255.
[14] W. Niblack, An introduction to digital image processing, Prentice-Hall, Englewood Cliffs, N.J., 1986, pp. 115–116.
[15] S.D. Yanowitz, A.M. Bruckstein, A new method for image segmentation, Comput. Vision, Graphics Image Process. 46 (1) (1989) 82–95.
[16] J. Sauvola, M. Pietikainen, Adaptive document image binarization, Pattern Recognition 33 (2) (2000) 225–236.
[17] Ø.D. Trier, A.K. Jain, Goal-directed evaluation of binarization methods, IEEE Trans. Pattern Anal. Mach. Intell. 17 (12) (1995) 1191–1201.
[18] M. Sezgin, B. Sankur, Survey over image thresholding techniques and quantitative performance evaluation, J. Electron. Imaging 13 (1) (2004) 146–168.
[19] X.S. Zhao, S.Z. Chen, Image segmentation based on global binarization and edge detection, J. Comput. Aided Des. Comput. Graphics 13 (2) (2001) 118–121.
[20] R. Cao, C.L. Tan, Q. Wang, P. Shen, Segmentation and analysis of double-sided handwritten archival documents, in: Proceedings of the Fourth IAPR Int'l Workshop Document Analysis Systems, December 2000, pp. 147–158.
[21] I. Blayvas, A. Bruckstein, R. Kimmel. Efficient computation of adaptive threshold surface for image binarization. Pattern Recognition 39 (1) (2006) 89–101.
[22] J. Canny, A computational approach to edge detection, IEEE Trans. Pattern Anal. Mach. Intell. 8 (6) (1986) 679–698.
[23] M. Sonka, V. Hlavac, R. Boyle, Image Processing, Analysis, and Machine Vision, second ed., Brooks/Cole, A Division of Thomson Learning, 1999.
[24] W.Y. Ma, B.S. Manjunath, Edgeflow: a technique for boundary detection and image segmentation, IEEE Trans. Image Process. 9 (8) (2000) 1375–1388.

About the Author—QIANG CHEN received B.Sc. degree in computer science and Ph.D. degree in Pattern Recognition and Intelligence System from Nanjing University of Science and Technology, China, in 2002 and 2007, respectively. Currently, he is a teacher with the School of Computer Science and Technology at the Nanjing University of Science and Technology. His main research topics are image segmentation, object tracking, image denoising, and image restoration. In particular, he is developing an intelligent image segmentation framework incorporating some prior information, such as shape, texture and motion, etc.

About the Author—QUAN-SEN SUN received his Ph.D. degree in pattern recognition and intelligence system from Nanjing University of Science and Technology (NUST), China, in 2006. He is a professor in the Department of Computer Science at NUST. He visited the Department of Computer Science and Engineering, The Chinese University of Hong Kong in 2004 and 2005, respectively. His current interests include pattern recognition, image processing, computer vision and data fusion.

About the Author—PHENG ANN HENG received B.Sc. degree from the National University of Singapore in 1985, and M.Sc. degree in computer science, M.A. degree in applied mathematics and Ph.D. degree in computer science, all from Indiana University, Bloomington, in 1987, 1988 and 1992, respectively. Currently, he is a Professor in the Department of Computer Science and Engineering, The Chinese University of Hong Kong (CUHK), Shatin. In 1999, he set up the Virtual Reality, Visualization and Imaging Research Centre at CUHK and serves as the Director of the Centre. He is also the Director of the CUHK Strategic Research Area in Computer Assisted Medicine, established jointly by the Faculty of Engineering and the Faculty of Medicine in 2000. His research interests include virtual reality applications in medicine, visualization, 3D medical imaging, user interface, rendering and modeling, interactive graphics and animation.

About the Author—DE-SHEN XIA received B.Sc. degree in Radiology of Nanjing Institute of Technology, China, in 1963, and Ph.D. degree in the Faculty of Science of Rouen University, France, in 1988.
Currently, he is a Professor in the Faculty of Computer Science and Technology, Nanjin University of Science and Technology (NJUST), Nanjing, China, Honorary Professor in ESIC/ELEC, Rouen, France and Research member in Computer Graphics Lab of CNRS, France. He is also Director of Image Recognition Lab in Nanjing University of Science and Technology, China. He is the direction member of National Remote Sensing Federation, China, and the direction member of Micro-Computer Application Association of Province Jiangsu, China. His research interests include image processing, analysis, and recognition, remote sensing, medical imaging and mathematics in imaging.